

Electron cyclotron effective mass in indium nitride

Michel Goiran,^{1,a)} Marius Millot,¹ Jean-Marie Poumirol,¹ Iulian Gherasoiu,² Wlodek Walukiewicz,³ and Jean Leotin¹

¹Laboratoire National des Champs Magnétiques Intenses (LNCMI)-CNRS UPR 3228, Université de Toulouse, 143 Avenue de Rangueil, 31400 Toulouse, France

²RoseStreet Labs Energy, 3701 E. University Drive, Phoenix, Arizona 85034, USA

³Materials Sciences Division, Lawrence Berkeley National Laboratory, Berkeley, California 94720, USA

(Received 3 September 2009; accepted 12 January 2010; published online 5 February 2010)

We report on cyclotron effective mass measurement in indium nitride epilayers grown on c-sapphire, using the thermal damping of Shubnikov-de-Haas oscillations obtained in the temperature range 2–70 K and under magnetic field up to 60 T. We unravel an isotropic electron cyclotron effective mass equal to $0.062 \pm 0.002m_0$ for samples having electron concentration near 10^{18} cm^{-3} . After nonparabolicity and polaron corrections we estimate a bare mass at the bottom of the band equal to $0.055 \pm 0.002m_0$. © 2010 American Institute of Physics. [doi:10.1063/1.3304169]

Among the group III-nitride materials, the electronic structure of InN is matter of continuing debate^{1–3} despite significant progress during the last decade in understanding the band structure, as the revision of its band gap energy from 1.8–2.1 eV to 0.7 eV.^{3,4} So far, band parameters are mostly derived from indirect methods of limited accuracy such as infrared reflectivity measurements. For instance, the values of the effective mass remain scattered in a wide range from 0.044 to $0.093m_0$.^{5–8} Moreover, a strongly anisotropic electronic structure of the bulk crystal has been claimed to explain Shubnikov-de-Haas (SdH) oscillations⁹ and magneto-optical properties.¹⁰ To date, the synthesis of highly pure InN single crystals remains a challenge and, in addition, most measurements are affected by the presence of an intrinsic low mobility surface and/or interface electron accumulation layer^{11,12} that opens parallel conduction channels. As a result, quite often the standard Hall effect measurements on thin film at low magnetic field do not provide accurate values for the bulk concentration^{13,14} and thus also the Fermi energy. This in turn may affect the effective mass determination.

In this letter, we report on the first measurement of the bulk electron cyclotron effective mass determined by Landau levels (LLs) spectroscopy; the most direct approach to measure effective masses. To derive the mass, we have used the temperature dependence of the SdH oscillation amplitudes measured under magnetic field up to 60 T in the temperature range 2–70 K. A set of three InN samples $1 \mu\text{m}$ thick having Hall concentrations 2×10^{18} , 3×10^{18} , and $6 \times 10^{18} \text{ cm}^{-3}$ has been investigated. We unveil an isotropic electron cyclotron effective mass equal to $0.062 \pm 0.002m_0$ but the highest doped sample exhibits a puzzling anisotropy.

Recently, the band structure of III-nitride was *ab initio* calculated in the entire Brillouin zone (BZ).¹⁵ Then, a $4 \times 4 \mathbf{k} \cdot \mathbf{p}$ hamiltonian that neglects the electron spin was parameterized to fit the band dispersion near the band extrema at the center of the BZ. The conduction band was found to be nonparabolic and slightly anisotropic with effective masses $m_{\parallel}^* = 0.065m_0$ along the *c*-axis and $m_{\perp}^* = 0.068m_0$ in a perpendicular direction. If one neglects the

anisotropy and the crystal field splitting related to the wurtzite symmetry, the conduction band is simply described a $2 \times 2 \mathbf{k} \cdot \mathbf{p}$ hamiltonian³ yielding the following dispersion relation:

$$E_c(k) = \frac{\hbar k^2}{2m_0} + \frac{E_g}{2} + \frac{1}{2} \sqrt{E_g^2 + \frac{4E_p \hbar^2 k^2}{2m_0}}, \quad (1)$$

where E_p is related to the optical matrix element and E_g is the band gap. The mass at the bottom of the band reads $m_0^* = (1/m_0 + E_p/E_g)^{-1}$. Given commonly accepted values of effective mass $m^* = 0.07m_0$, and band gap $E_g = 0.69 \text{ eV}$,^{2,3} the E_p parameter takes the value $E_p = 9.3 \text{ eV}$.

The epilayers were grown by plasma-assisted molecular beam epitaxy on a 300 nm thick GaN buffer layer initially grown at 720 °C on c-plane sapphire substrates. The wafer temperature was then reduced in the range 460–590 °C to grow the InN layer. The unintentional doping due to nitrogen vacancies was controlled by employing an adaptive deposition technique¹⁶ known as metal modulation epitaxy. Samples were characterized using photoluminescence and Hall-measurements at room and liquid-nitrogen temperature. For high field measurements Hall bar geometry samples were processed. The temperature was varied from 2 to 80 K. For each temperature, a magnetic field pulse up to 60 T allowed to measure the magnetoresistance using standard ac lock-in technique. The crystal can be rotated from $B \parallel c$ -axis to $B \perp c$ -axis.

A strong magnetic field quantizes the energy states of the electrons into LLs. In the $2 \times 2 \mathbf{k} \cdot \mathbf{p}$ framework, we shall use Eq. (1) to calculate the LLs energies of electrons in a magnetic field taking into account the quantization rule $k^2 = (2N+1)(eB/\hbar)$. This gives equally spaced levels $E_N(B) = (N+1/2)\hbar eB/m_c^*$ at low magnetic field and low energy and unevenly spaced LLs at higher energy and magnetic field reflecting the band nonparabolicity. Then the electron cyclotron effective mass m_c^* is deduced from LLs separation $\hbar eB/m_c^*$. The SdH oscillations of the longitudinal resistance R_{xx} under applied magnetic field occur when LLs cross E_F during the magnetic field sweep. However, oscillations appear only in high mobility samples and at high magnetic fields such that the collision time exceeds the cyclotron period, that means $B > 10^4/\mu$, i.e., $B > 10 \text{ T}$ is required when

^{a)}Electronic mail: goiran@lncmpi.org.

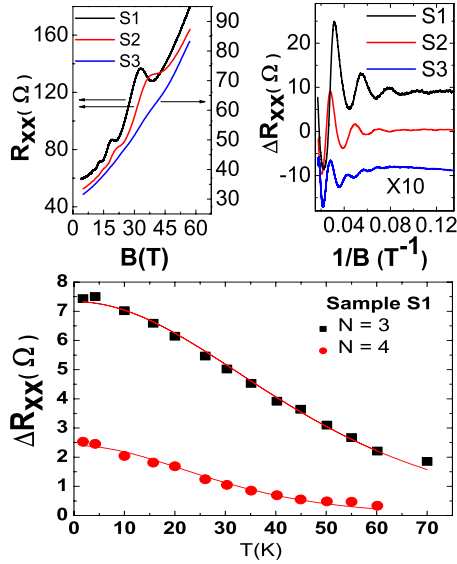


FIG. 1. (Color online) (a) Resistance vs magnetic field parallel to the c -axis for the three samples S1, S2 (left scale), and S3 (right scale) measured at 2 K. (b) SdH oscillations vs reciprocal magnetic field obtained from the magnetoresistance curves. Note that all curves have been shifted vertically for clarity. (c) Temperature dependence of the oscillation amplitude for SdH peaks with $N=3$ and $N=4$ LLs numbers (sample S1).

$\mu=1000$ cm²/V s. In addition, the samples concentration must be homogeneous enough to reduce Fermi level fluctuations that would wash out the oscillations toward higher magnetic fields. As a matter of fact, in InN, despite concentration inhomogeneity and low mobility of bulk and surface electrons, measurements of SdH oscillations periods at high enough magnetic fields, tilted away from c -axis by an angle θ , give a unique opportunity to measure the bulk Fermi surface cross sections anisotropy and characterize surface electrons. Indeed, surface electrons are easily distinguished from bulk electrons since their SdH period increases as $1/B \cos \theta$.

Figure 1(a) shows the longitudinal resistance R_{xx} of the three samples, S1, S2 and S3, at 2 K as a function of the magnetic field oriented along the c -axis. Hall concentration are, respectively, of 2×10^{18} , 3.6×10^{18} , and 6×10^{18} cm⁻³ (see Table I). Figure 1(b) shows the oscillatory part ΔR_{xx} of the resistance as a function of the reciprocal magnetic field, after subtracting a parabolic background. We find a single SdH series for magnetic field parallel to the c -axis in contrast with Ref. 9 that reports an additional SdH series at higher frequency for a sample with a similar Hall concentration $n_H=2.2 \times 10^{18}$ cm⁻³. This single series keeps the same period below 22 T when the field direction is tilted away from the c -axis (see Fig. 2), hence it behaves like the main series of Ref. 9 and consequently, accounts for an isotropic bulk Fermi surface as stated in this earlier work. Surface electrons SdH oscillations are not evidenced in the measured 60 T field

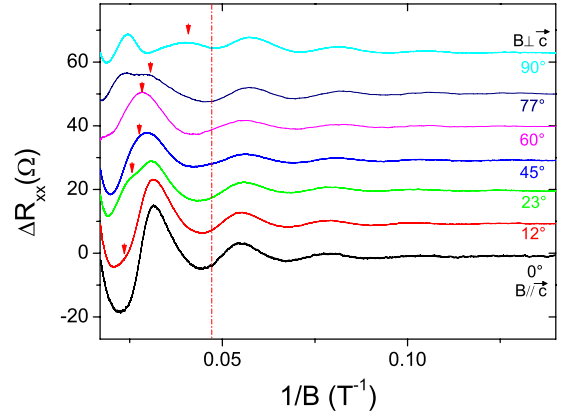


FIG. 2. (Color online) Angular dependence of R_{xx} vs reciprocal magnetic field for sample S1. The red arrows show the additional single peak that adds up to the SdH oscillation, the red dot line show the position of $(1/22)T^{-1}$.

range with $B \parallel c$ -axis, likely because of low electron mobility and/or concentration inhomogeneity.

However, one should mention now a peculiar feature that occurs above 22 T when the magnetic field is parallel to the layer ($B \perp c$). An additional single peak (see arrows on Fig. 2) adds up to the SdH series. As the in-plane magnetic field is reduced by tilting the sample, this peak moves toward higher magnetic fields and disappears. We believe this extra peak is a signature of the two-dimensional structure of the accumulation layer and is caused by the upper electrical subband crossing the Fermi level. Indeed, the magnetic field shifts upwards this subband by a diamagnetic contribution to the binding energy.¹⁷

The well established Lifshitz–Kosevich model allows us to determine accurately the cyclotron effective mass from the thermal damping of the SdH oscillations without any fitting parameters.¹⁸ At a given maximum of the ΔR_{xx} , i.e., a fixed value of the magnetic field, the thermal decay of this SdH oscillation amplitude is determined by the cyclotron effective mass following:

$$\Delta R_{xx}(T, B) \propto T / \sinh\left(\frac{2\pi^2 k_B T m^*}{eB\hbar}\right). \quad (2)$$

Such a decay for peaks measured in the temperature range 2–70 K at Landau numbers $N=3$ and 4 for B perpendicular to the c -axis is shown for the sample S1, in the Fig. 1(c). The effective mass is then deduced as an average of the values obtained from the thermal damping fit of the different maxima. One finds a constant isotropic mass at lowest concentrations, but, in the highest doped sample, a puzzling increase in the mass by 30% occurs when B is parallel to the epilayer. In this case, the magnetic field should probe an elliptical cyclotron orbit with a cyclotron mass $\sqrt{m_{\perp}^* m_{\parallel}^*}$.

TABLE I. Results summary: Hall concentration, SdH concentration, Hall mobility, and cyclotron effective masses with $B \perp c$ -axis and $B \parallel c$ -axis. Fermi levels are calculated using the nonlinear band dispersion relation (1).

Sample	n_H at 300 K (10^{18} cm ⁻³)	n_{SdH} (10^{18} cm ⁻³)	μ_H at 300 K (cm ² /V s)	E_F bulk (meV)	$\sqrt{(m_{\perp} m_{\parallel})/m_0^2}$, ($B \perp c$ -axis)	m_{\perp}/m_0 , ($B \parallel c$ -axis)
S1	2	1.51	1900	63	0.062 ± 0.001	0.062 ± 0.001
S2	3.6	1.86	900	72	0.062 ± 0.001	0.062 ± 0.001
S3	6	4.25	800	119	0.082 ± 0.001	0.064 ± 0.001

Given the measured transverse mass $m_{\perp}^* = 0.064m_0$, the effective mass m_{\parallel}^* along the c -axis would be as high as $0.105m_0$. Such a mass increase, neither predicted by *ab initio* calculations nor by the $\mathbf{k} \cdot \mathbf{p}$ model, remains unexplained and calls for more investigations of higher doped epilayers.

These effective masses have been measured at the Fermi level, we now proceed to derive the values at the bottom of the band. Taking into account nonparabolicity corrections the bottom band effective mass becomes

$$m_0^* = m^* \left[1 - \frac{E_F}{E_g} \left(\frac{m^*}{m_0} - 1 \right)^2 \right] \quad (3)$$

and takes the value $m_0^* = 0.057m_0$.

Another correction to be done is the polaron contribution. Assuming an isotropic electron-LO phonon coupling constant in InN, $\alpha = 0.22$,¹⁹ the polaron mass m_p^* is given by the following:

$$\frac{m_p^*}{m^*} = (1 + \alpha/12)/(1 - \alpha/12). \quad (4)$$

One finds a 4% correction that finally gives the bare mass at the bottom of the conduction band equal to $m_0^* = 0.055 \pm 0.002m_0$. The band parameter E_p in the dispersion relation (1) thus becomes $E_p = 12$ eV, with $E_g = 0.69$ eV.

To summarize, electron cyclotron effective mass of InN on c -sapphire substrate is obtained from the temperature dependence of SdH oscillations. An isotropic cyclotron effective mass equal to $0.062 \pm 0.002m_0$ is measured for samples having bulk electron concentration in the range $1 \times 10^{18} - 4 \times 10^{18}$ cm⁻³. After nonparabolicity and polaron corrections the effective mass at the bottom of the band becomes $m_0^* = 0.055m_0 \pm 0.002$.

Authors acknowledge helpful discussions with P. Rinke, M. Winkelkemper, and D. Charrier. Part of this work was supported by EuroMagNET II.

- ¹J. Wu, *J. Appl. Phys.* **106**, 011101 (2009).
- ²I. Vurgaftman and J. Meyer, *J. Appl. Phys.* **94**, 3675 (2003).
- ³J. Wu, W. Walukiewicz, K. M. Yu, J. W. Ager III, E. E. Haller, H. Lu, W. Schaff, Y. Saiton, and Y. Nanishi, *Appl. Phys. Lett.* **80**, 3967 (2002).
- ⁴T. L. Tansley and C. P. Foley, *J. Appl. Phys.* **59**, 3241 (1986).
- ⁵J. Wu, W. Walukiewicz, W. Shan, K. M. Yu, J. W. Ager III, E. E. Haller, H. Lu, and W. J. Schaff, *Phys. Rev. B* **66**, 201403(R) (2002).
- ⁶S. P. Fu and Y. F. Chen, *Appl. Phys. Lett.* **85**, 1523 (2004).
- ⁷T. Inushima, M. Higashiwaki, and T. Matsui, *Phys. Rev. B* **68**, 235204 (2003).
- ⁸G. Pettinari, A. Polimeni, M. Capizzi, J. H. Blokland, P. C. M. Christensen, J. C. Maan, V. Lebedev, V. Cimalla, and O. Ambacher, *Phys. Rev. B* **79**, 165207 (2009).
- ⁹T. Inushima, M. Higashiwaki, and T. Matsui, *Phys. Rev. B* **72**, 085210 (2005).
- ¹⁰T. Hofmann, V. Darakchieva, B. Monemar, H. Lu, W. J. Schaff, and M. Schubert, *J. Electron. Mater.* **37**, 611 (2008).
- ¹¹H. Lu, W. J. Schaff, L. F. Eastman, and C. E. Stutz, *Appl. Phys. Lett.* **82**, 1736 (2003).
- ¹²L. Colakerol, T. D. Veal, H.-K. Jeong, L. Plucinski, A. DeMasi, T. Learmonth, P.-A. Glans, S. Wang, Y. Zhang, L. F. J. Piper, P. H. Jefferson, A. Fedorov, T.-C. Chen, T. D. Moustakas, C. F. McConville, and K. E. Smith, *Phys. Rev. Lett.* **97**, 237601 (2006).
- ¹³S. X. Li, K. M. Yu, J. Wu, R. E. Jones, W. Walukiewicz, J. W. Ager III, W. Shan, E. E. Haller, H. Lu, and W. J. Schaff, *Phys. Rev. B* **71**, 161201(R) (2005).
- ¹⁴T. A. Komissarova, M. A. Shakhov, V. N. Jmerik, T. V. Shubina, R. V. Parfeniev, S. V. Ivanov, X. Wang, and A. Yoshikawa, *Appl. Phys. Lett.* **95**, 012107 (2009).
- ¹⁵P. Rinke, M. Winkelkemper, A. Qteish, D. Bimberg, J. Neugebauer, and M. Scheffler, *Phys. Rev. B* **77**, 075202 (2008).
- ¹⁶T. Gherasoiu, M. O'Steen, T. Bird, D. Gotthold, A. Chandolu, D. Y. Song, S. X. Xu, M. Holtz, S. A. Nikishin, and W. J. Schaff, *J. Vac. Sci. Technol. A* **26**, 399 (2008).
- ¹⁷H. Reisinger and F. Koch, *Surf. Sci.* **170**, 397 (1986).
- ¹⁸I. M. Lifshitz and A. M. Kosevich, *Sov. Phys. JETP* **2**, 636 (1955).
- ¹⁹Z. W. Yan, S. L. Ban, and X. X. Liang, *Eur. Phys. J. B* **43**, 339 (2005).